

Supplementary Figure S1. Hyper-stable p53(A347D) preferentially forms dimers and may not heterotetramerize with WT p53

(A) The frequency of p53 germline mutations relative to the length of the domain in which the mutation occurs was calculated from data obtained from The *TP53* Database (R20, 2019). Domain abbreviations are defined thus: TAD1 – Transactivation Domain 1 (1-42), TAD2 – Transactivation Domain 2 (43-61), PRD – Proline-Rich Domain (42-98), DBD – DNA-binding domain (101-292), NLS – Nuclear Localization Signal (316-323), OD – Oligomerization Domain (324-356), RD (362-393).

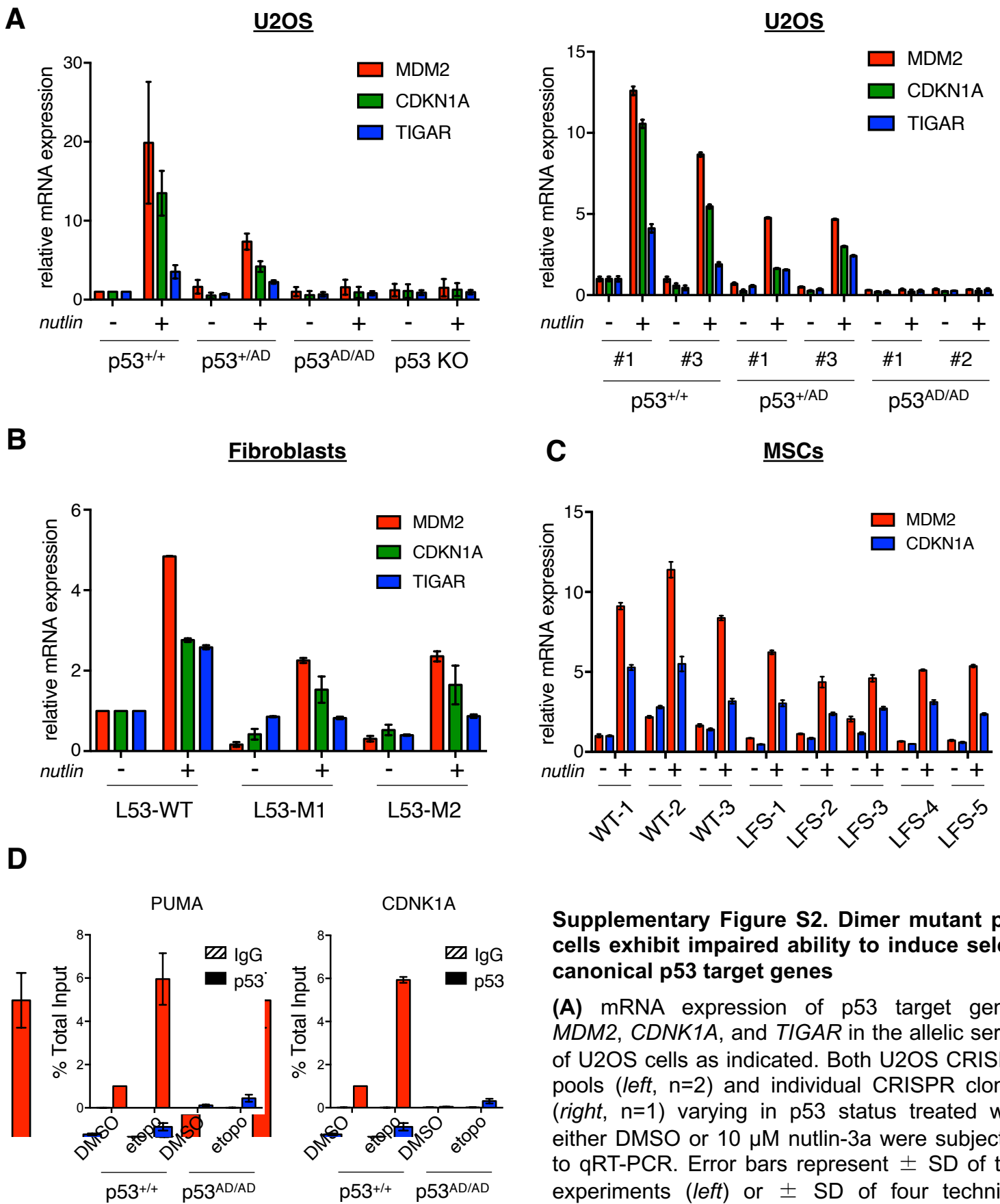
(B) Plasmids expressing WT p53, p53(A347D), p53-A347T, or p53-L330A were transfected into H1299 lung adenocarcinoma cells. Protein lysates extracted were incubated in the presence or absence of 0.05% glutaraldehyde for 20 min at room temperature (RT) and subjected to immunoblot analysis with a monoclonal p53 antibody (DO1/1801) to detect p53 oligomeric species. Red asterisk denotes the likely tetrameric species.

Supplementary Figure S1. Hyper-stable p53(A347D) preferentially forms dimers and may not heterotetramerize with WT p53

(C) Plasmids expressing Flag-tagged WT p53, HA-tagged p53(A347D), and/or HA-tagged WT p53 were transfected into U2OS p53 KO cells according to the indicated combinations. Protein lysates were isolated and subjected to immunoprecipitation with anti-FLAG antibody followed by immunoblotting with either anti-HA or anti-FLAG antibodies.

(D) Single CRISPR clones of U2OS cells varying in p53 status as indicated were treated with 10 μ M nutlin-3a for 24 h and then lysed. Protein lysates were then subjected to immunoblot analysis with antibodies against indicated proteins.

(E) Following the addition of cycloheximide (100 μ g/mL), U2OS cells expressing WT p53, p53^{+AD}, and p53^{AD/AD} were harvested at the indicated times. Cell lysates were then subjected to immunoblotting. Left and right blots represent two biologically independent experiments.



Supplementary Figure S2. Dimer mutant p53 cells exhibit impaired ability to induce select canonical p53 target genes

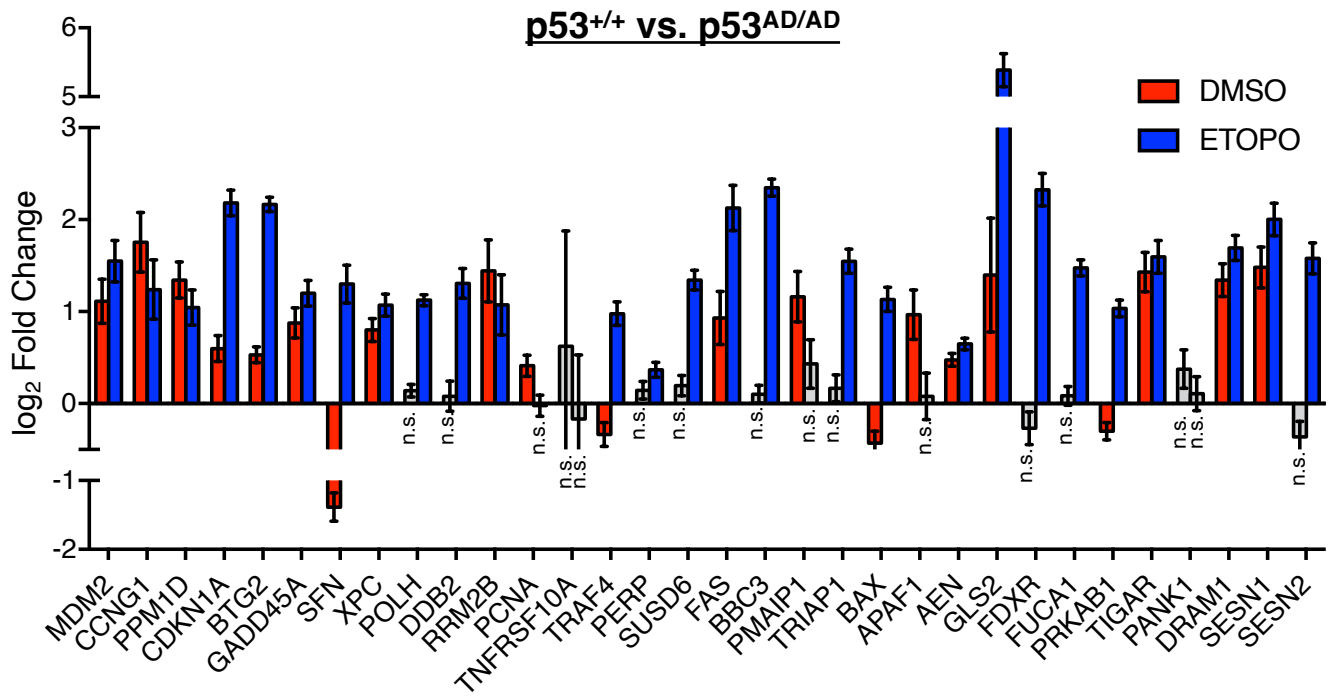
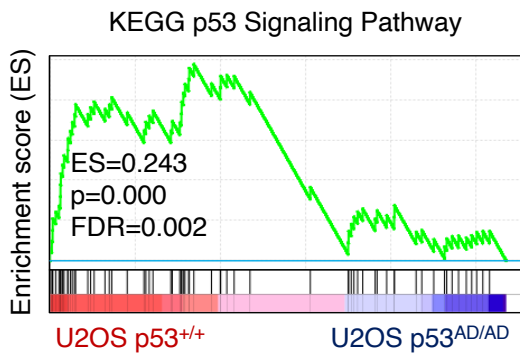
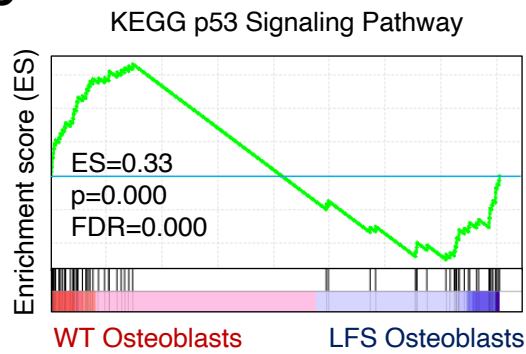
(A) mRNA expression of p53 target genes *MDM2*, *CDKN1A*, and *TIGAR* in the allelic series of U2OS cells as indicated. Both U2OS CRISPR pools (left, n=2) and individual CRISPR clones (right, n=1) varying in p53 status treated with either DMSO or 10 μ M nutlin-3a were subjected to qRT-PCR. Error bars represent \pm SD of two experiments (left) or \pm SD of four technical replicates (right).

(B) mRNA expression of p53 target genes *MDM2*, *CDKN1A*, and *TIGAR* in patient-derived dermal fibroblasts varying in p53 status treated with either DMSO or 10 μ M nutlin-3a was assessed by qRT-PCR. Error bars represent \pm SEM of two experiments.

Supplementary Figure S2. Dimer mutant p53 cells exhibit impaired ability to induce select canonical p53 target genes

(C) mRNA expression of p53 target genes *MDM2* and *CDNK1A* in single clones of either WT or LFS mesenchymal stem cells (MSCs) treated with either DMSO or 10 μ M nutlin-3a was assessed by qRT-PCR. Error bars represent \pm SEM of three experiments.

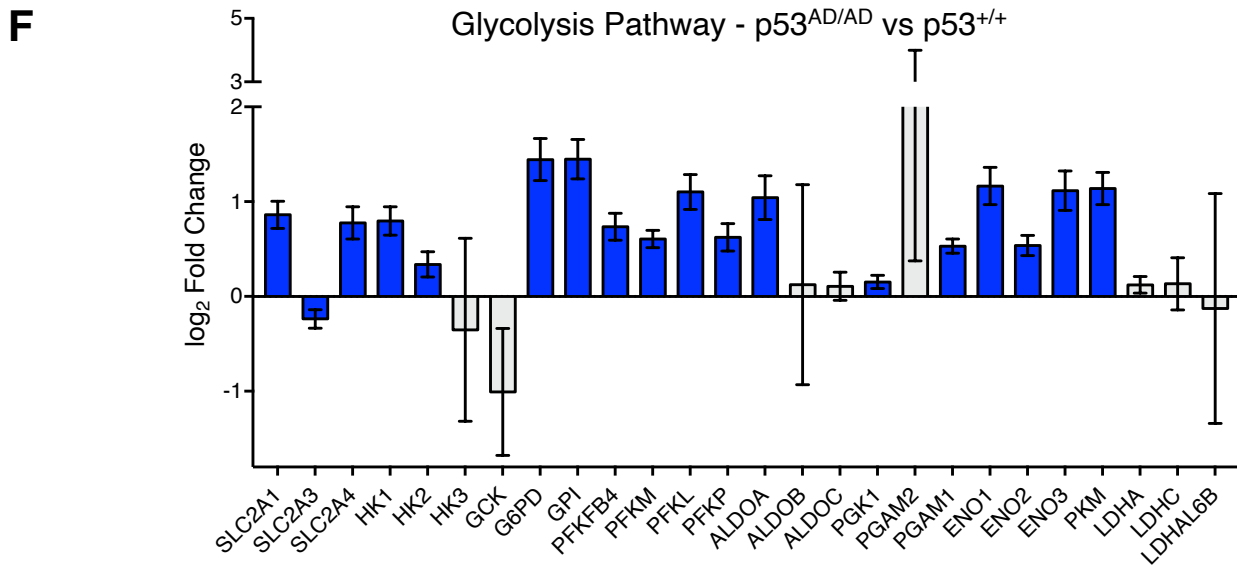
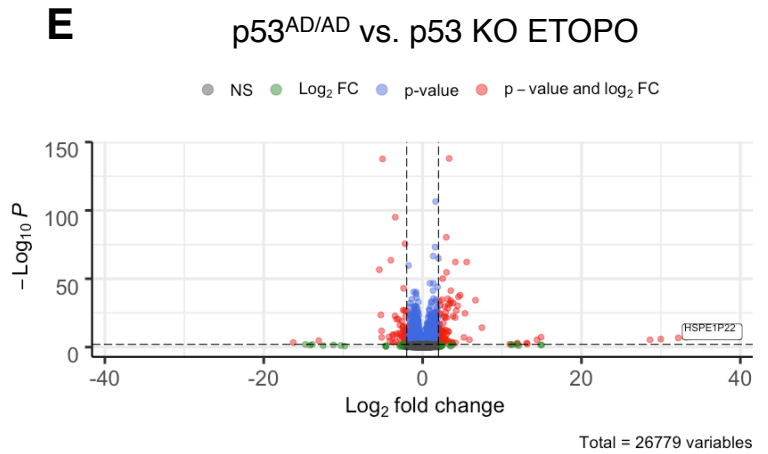
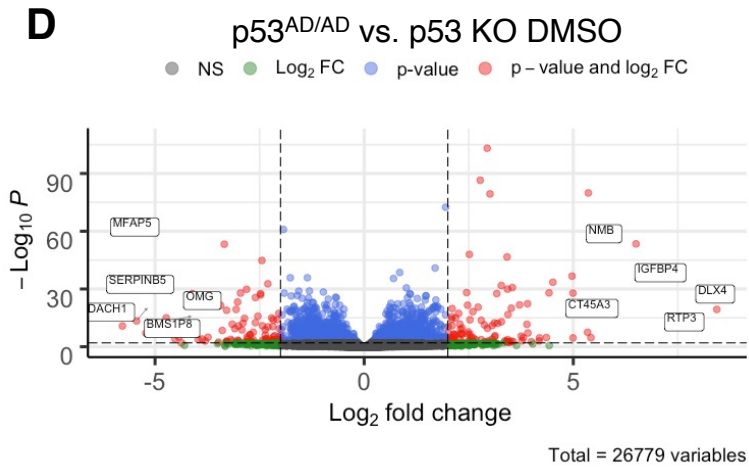
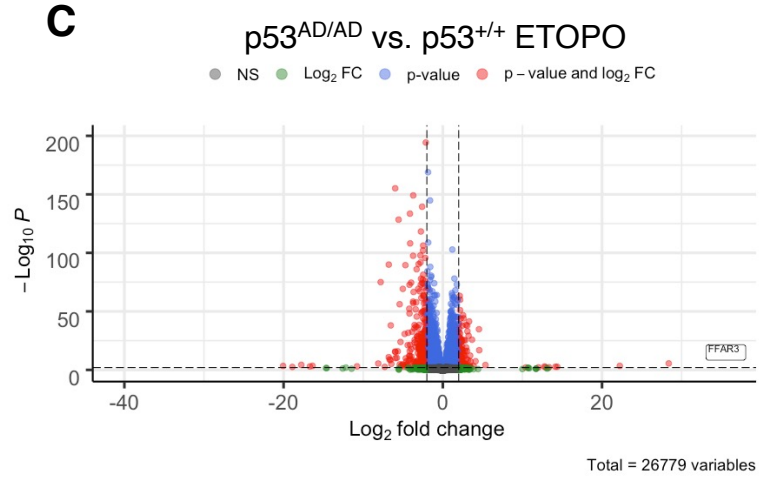
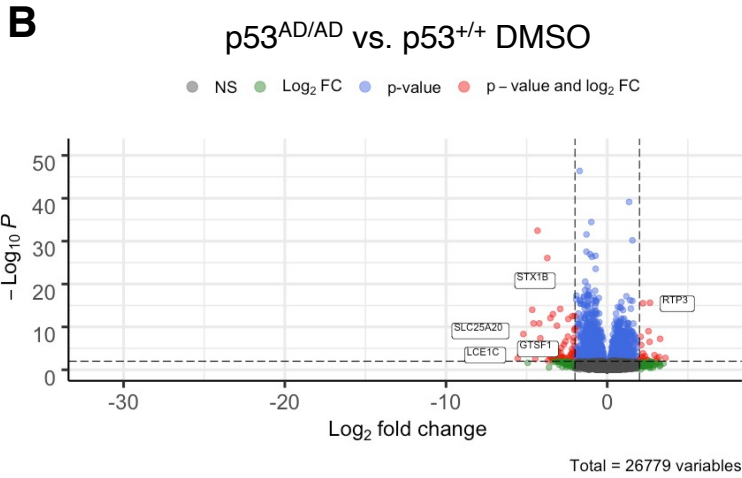
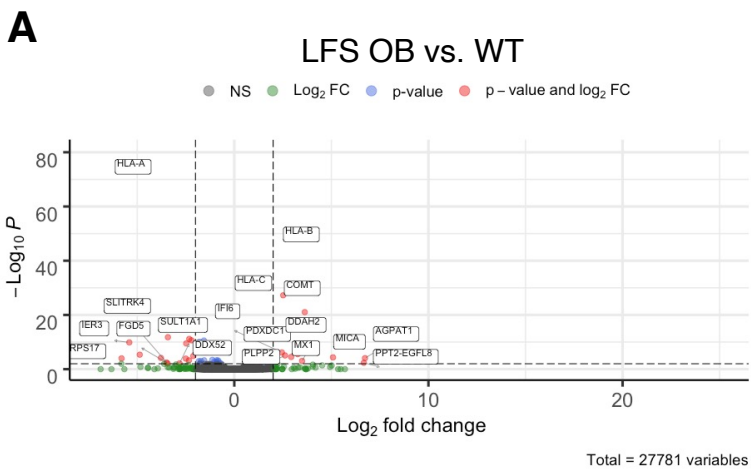
(D) U2OS p53^{+/+} and p53^{AD/AD} cells were seeded in 15 cm plates and treated for 24 h with either DMSO or 20 μ M etoposide. Cells were harvested, crosslinked, and subjected to ChIP-qPCR to assess endogenous p53 binding on indicated promoters. Data represent a minimum of 3 biologically independent experiments and were normalized within each experiment to the p53 signal in DMSO-treated U2OS parental condition. Bars represent mean \pm SEM.

A**B****C**

Supplementary Figure S3. Transcriptional profiling reveals decreased expression of canonical p53 targets in dimeric mutant p53-bearing cells

(A) Differential gene expression of canonical p53 targets in p53^{+/+} relative to p53^{AD/AD} cells treated with DMSO or 20 μ M etoposide are shown as log₂ fold change. Data represent mean \pm SEM for four technical replicates. Bars in color represent log₂ fold change values with a p<0.05.

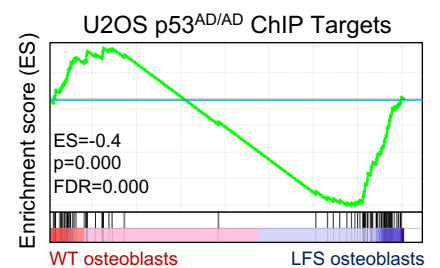
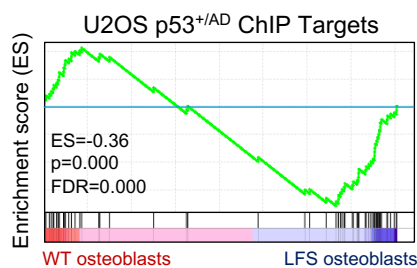
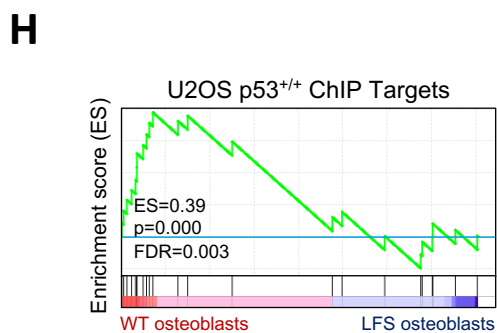
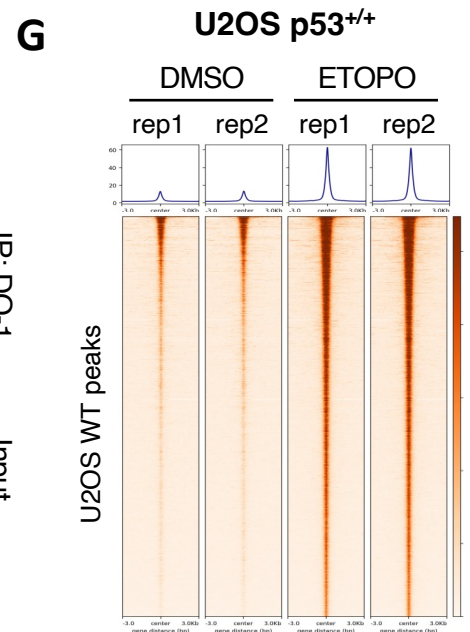
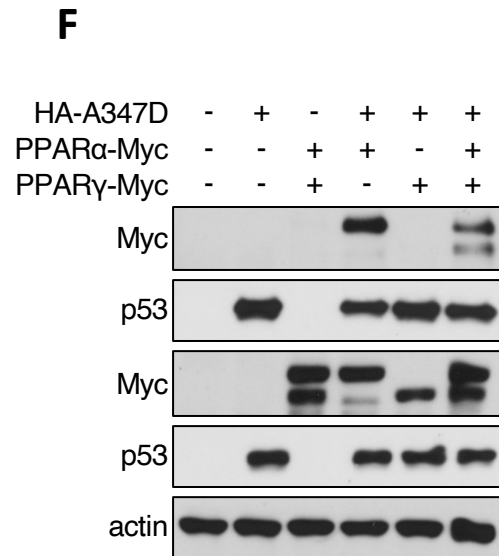
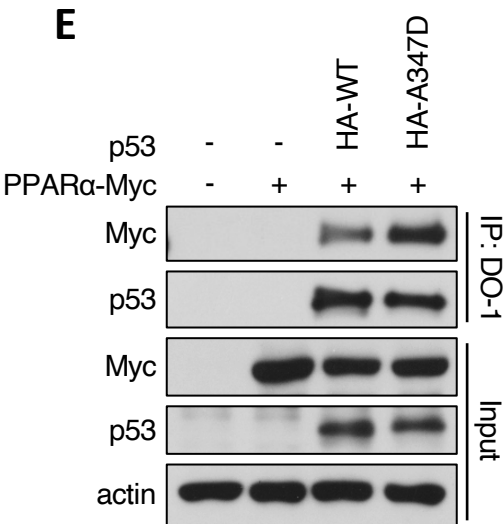
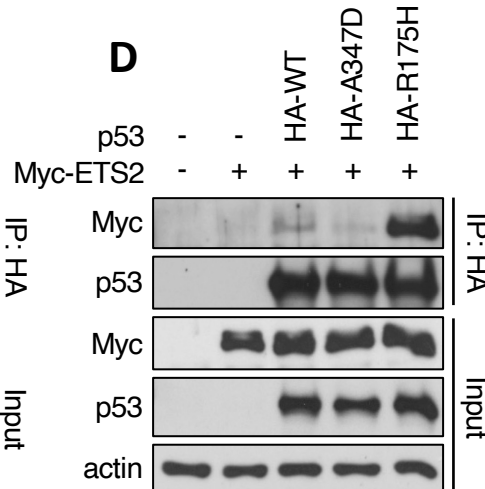
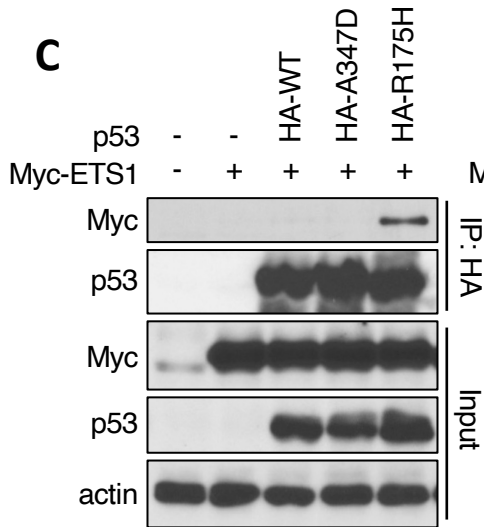
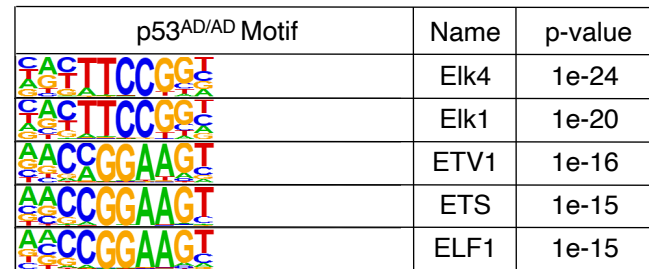
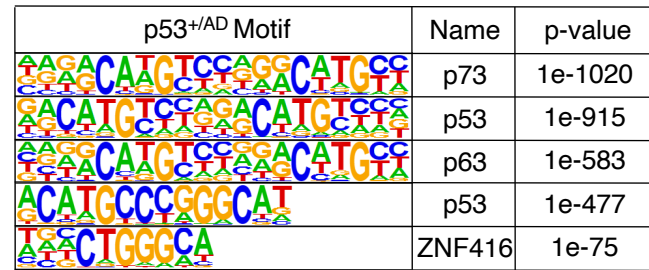
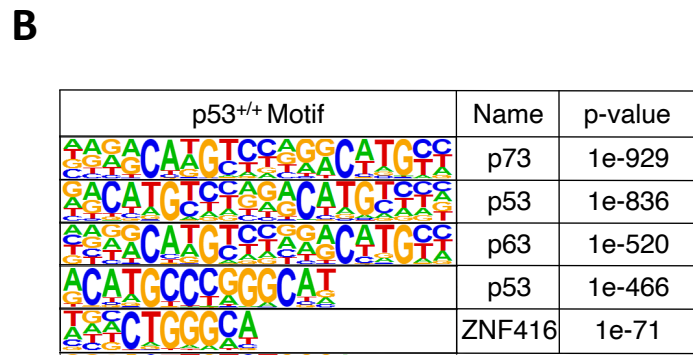
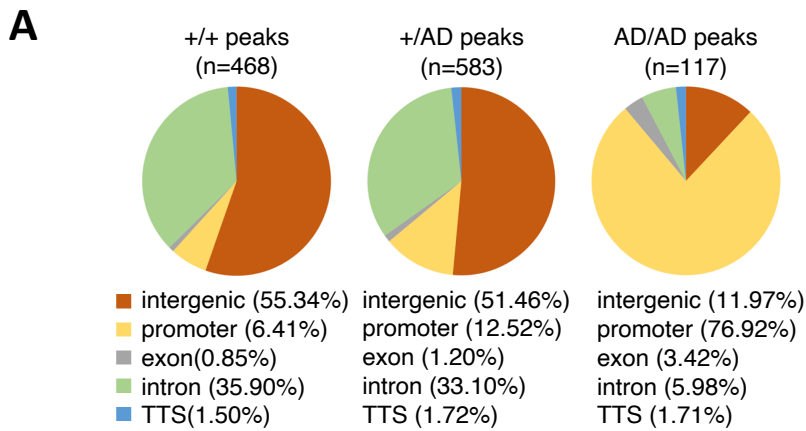
(B-C) Enrichment plots of GSEA results demonstrating significant enrichment of KEGG p53 signaling pathway genes in U2OS p53^{+/+} cells and WT osteoblasts relative to U2OS p53^{AD/AD} cells and LFS osteoblasts, respectively.



Supplementary Figure S4. Dimeric mutant p53 cells exhibit an altered transcriptional profile

(A-E) Volcano plots demonstrating differential gene expression in dimeric mutant p53-bearing cells relative to wild-type or p53 KO cells from either two biologically independent experiments in U2OS cells or one experiment in osteoblasts. Dots in red represent genes with a p -value of <0.01 and a \log_2 fold change $>|2|$. Dots in blue represent genes significantly differentially expressed (p -value <0.01). Dots in green represent genes that meet the \log_2 fold change cutoff but not the significance threshold. Dots in grey are not significantly altered.

(F) Differential gene expression of glycolysis pathway genes in p53^{AD/AD} U2OS cells relative to p53^{+/+} U2OS cells shown as \log_2 fold change. Data represent mean \pm SEM for four technical replicates. Bars in blue represent \log_2 fold change values with a $p<0.05$. Statistical significance was assessed by two-tailed t -test. *** $p<0.001$, ** $p<0.01$, * $p<0.05$



Supplementary Figure S5. Dimeric mutant p53 associates with novel genomic loci and binds PPAR proteins

(A) Venn diagrams illustrate the genomic distribution of p53 binding sites in p53^{+/+}, p53^{+/^{AD}}, and p53^{AD/AD} U2OS cells.

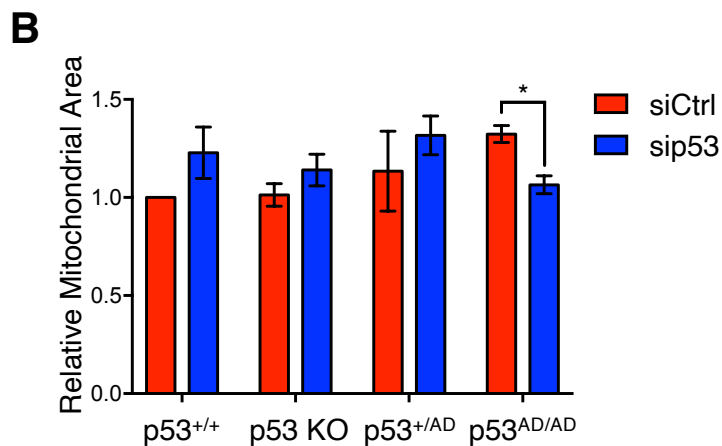
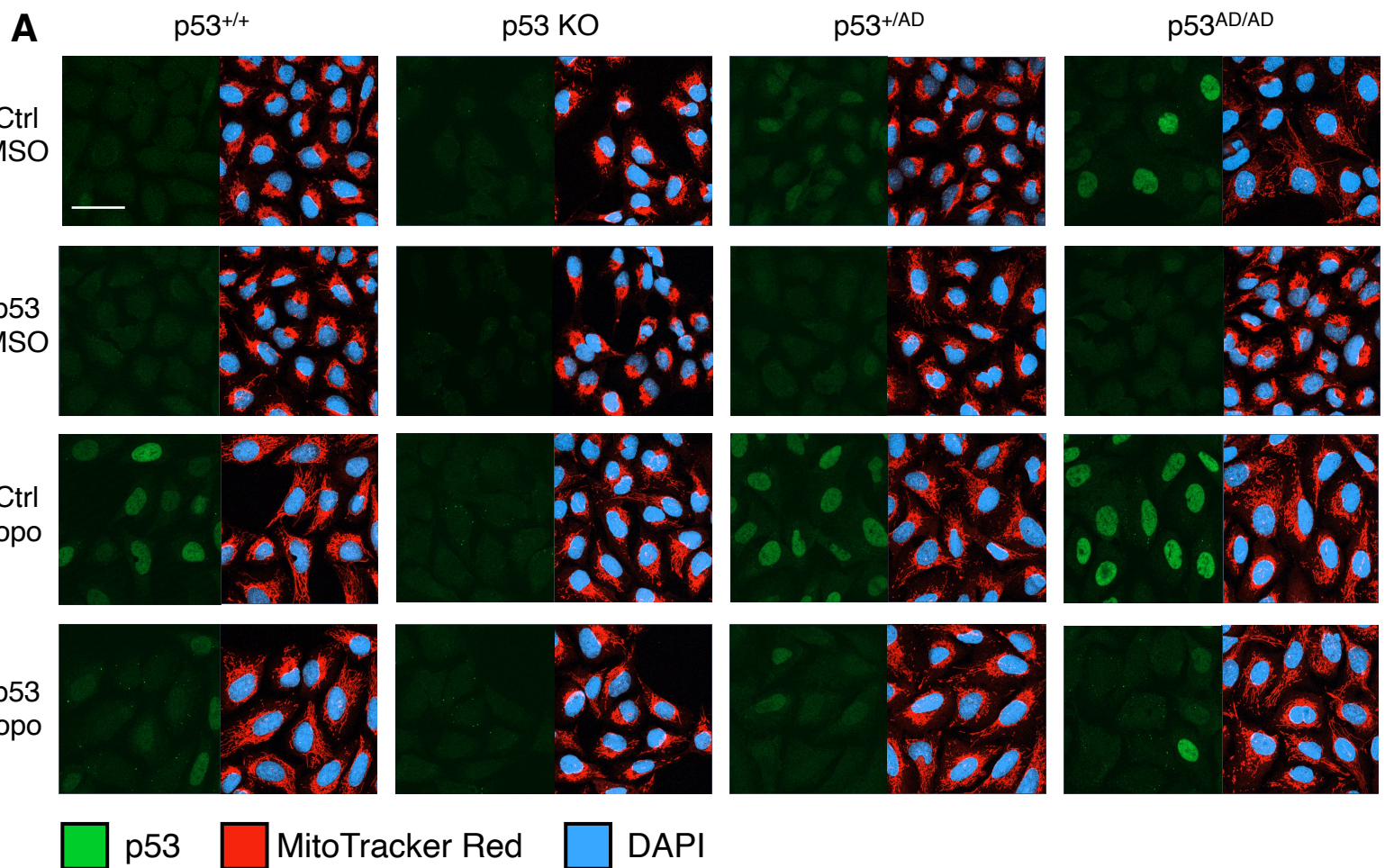
(B) Tables depict binding motifs identified by *de novo* motif enrichment analysis in p53^{+/+}, p53^{+/^{AD}}, and p53^{AD/AD} U2OS cells.

(C-D) H1299 cells were co-transfected with the empty vector pcDNA3, HA-WT p53, HA-p53(A347D), or HA-p53(R175H) and myc-ETS1 or myc-ETS2 plasmids according to indicated combinations. Protein lysates were immunoprecipitated with anti-HA agarose beads and subjected to immunoblot analysis with indicated antibodies.

(E-F) U2OS p53 KO cells were co-transfected with the empty vector pcDNA3, HA-WT p53 or HA-p53(A347D) and myc-DDK-PPAR α and/or myc-DDK-PPAR γ plasmids according to indicated combinations. Protein lysates were immunoprecipitated with anti-p53 (DO-1) and subjected to immunoblotting with indicated antibodies.

(G) Heatmaps demonstrate wild-type p53 binding to 1-kb genomic loci surrounding peaks identified in p53^{+/+} U2OS cells upon treatment with DMSO or 20 μ M etoposide for 24 h.

(H) GSEA plots demonstrating enrichment of U2OS p53^{+/+}, p53^{+/^{AD}}, or p53^{AD/AD} ChIP targets in LFS osteoblasts vs. WT osteoblasts expression datasets.

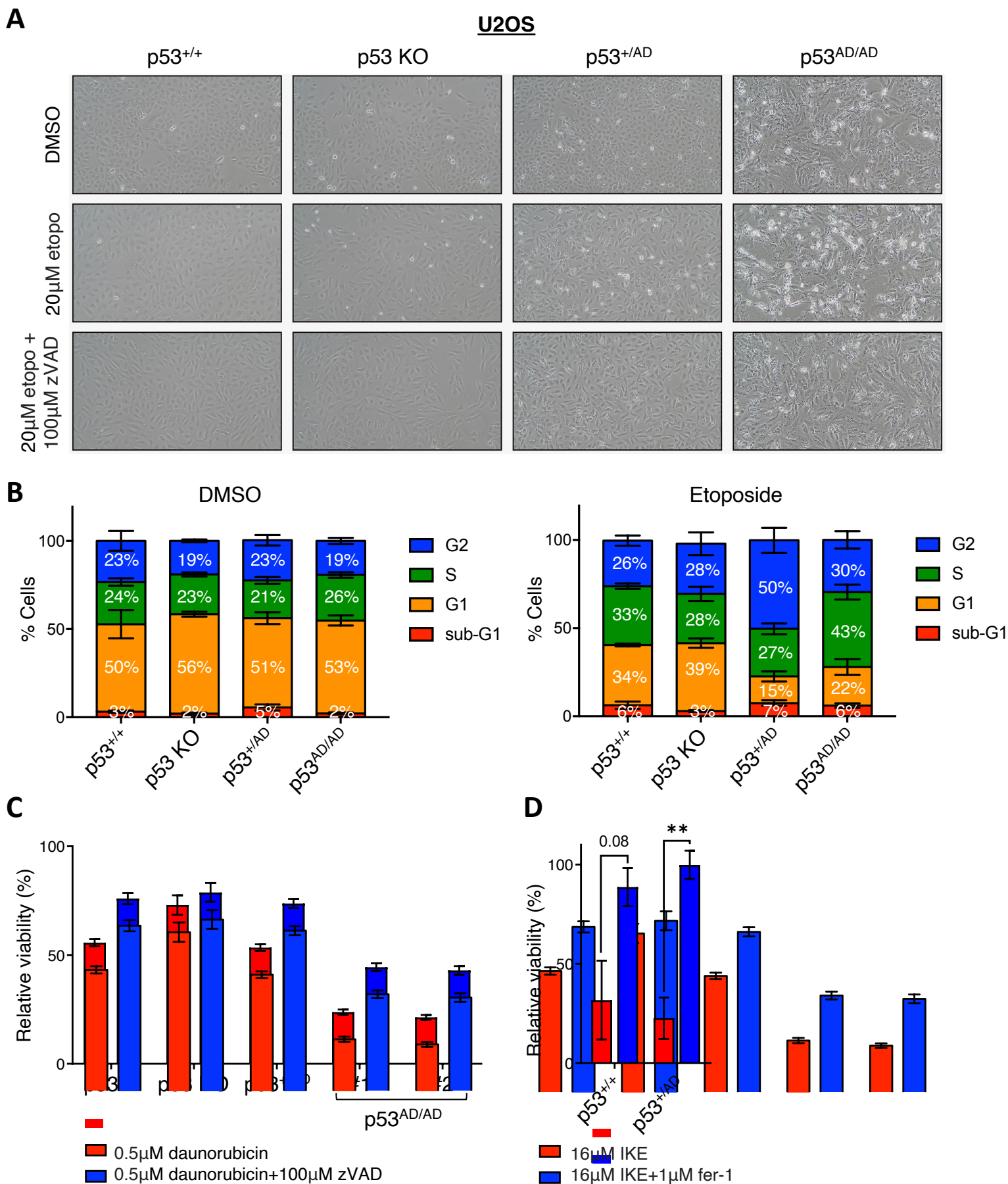


Supplementary Figure S6. Dimeric mutant p53 promotes mitochondrial network aberration

(A) U2OS cells with p53^{+/+}, p53 KO, p53^{+/AD}, and p53^{AD/AD} were transfected with 25 nM of either a non-targeting siRNA pool or siRNA pool against p53 for 48 h and then were split onto coverslips and let adhere overnight. Cells were then treated with 20 μ M etoposide (etopo) for 24 h, fixed with 4% paraformaldehyde, and stained with an anti-p53 antibody (green), MitoTracker Red CMXRos (red), and DAPI (blue).

(B) Quantification of mitochondrial area per cell normalized to the U2OS p53^{+/+} siCtrl DMSO condition. Bars represent the mean \pm SEM of three biologically independent experiments. (n=3, 7-12 images captured per group).

Statistical significance was assessed by two-tailed *t*-test. **p*<0.05



Supplementary Figure S7. Mutant p53 U2OS cells experience elevated growth arrest and death upon topoisomerase-II inhibition

(A) U2OS cells varying in p53 status (p53^{+/+}, p53 KO, p53^{+AD}, and p53^{AD/AD}) were treated with DMSO, 20 μM etoposide (etopo), or 20 μM etopo + 100 μM zVAD-FMK (zVAD) for 48 h and visualized by brightfield microscopy.

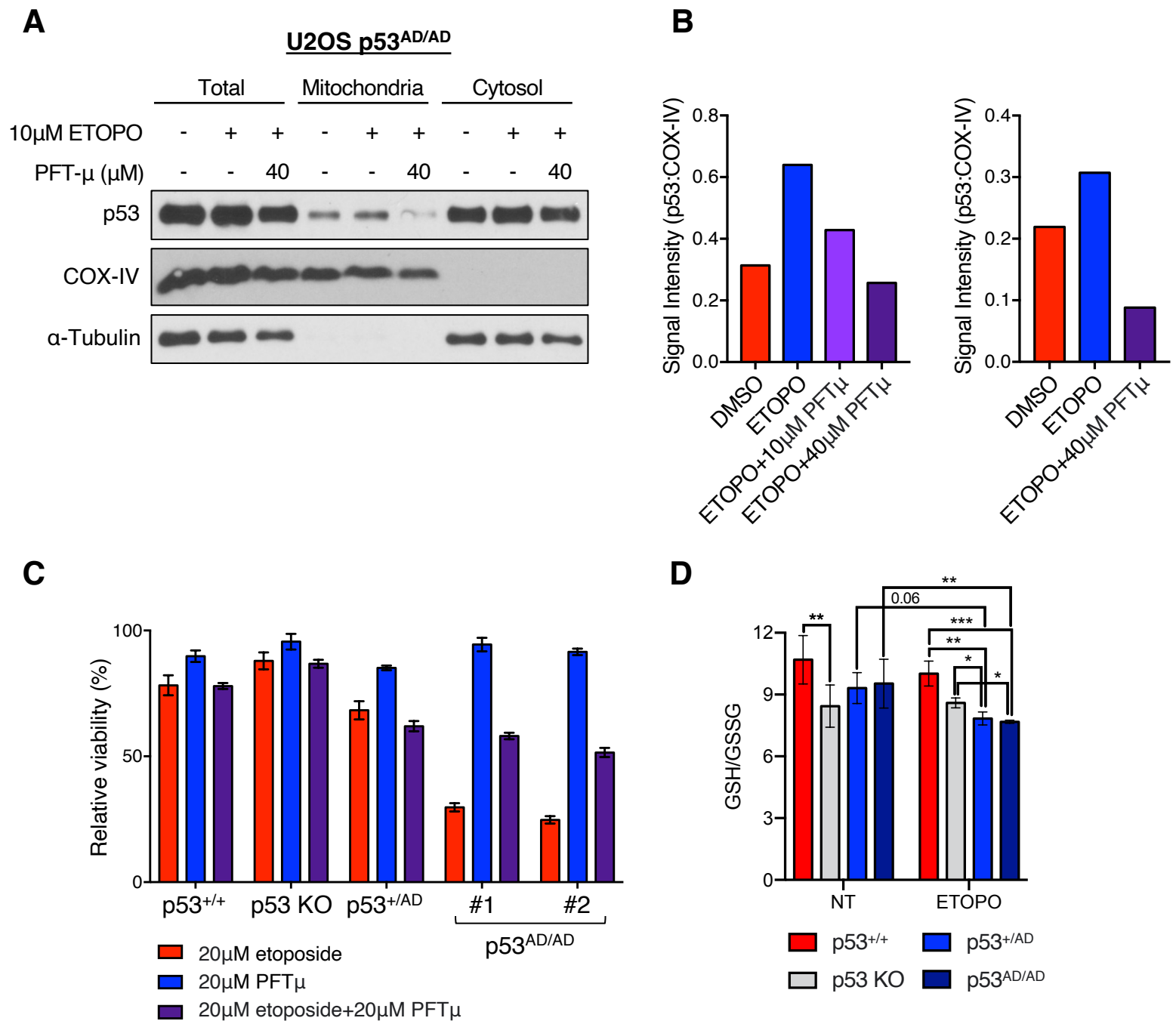
Supplementary Figure S7. Mutant p53 U2OS cells experience elevated growth arrest and death upon topoisomerase-II inhibition

(B) Cell cycle profiles of U2OS cells varying in p53 status following treatment with either DMSO or 20 μ M etoposide for 24 h were determined by PI staining followed by flow cytometric analysis. Bars represent mean \pm SEM of five independent experiments (n=5).

(C) Viability of U2OS parental (p53^{+/+}) and individual U2OS CRISPR clones treated for 72 h with DMSO, 0.5 μ M daunorubicin, and 0.5 μ M daunorubicin + 100 μ M zVAD-FMK (zVAD) was measured via neutral red uptake and normalized to the DMSO control for each cell line. Bars represent mean \pm SEM of three independent experiments (n=3).

(D) Viability of p53^{+/+} and p53^{+AD} U2OS cells treated with 16 μ M IKE or 16 μ M IKE + 1 μ M ferrostatin-1 for 48 h. Bars represent mean \pm SEM of three independent experiments (n=3).

Statistical significance was assessed by two-tailed *t*-test. **p<0.01, *p<0.05



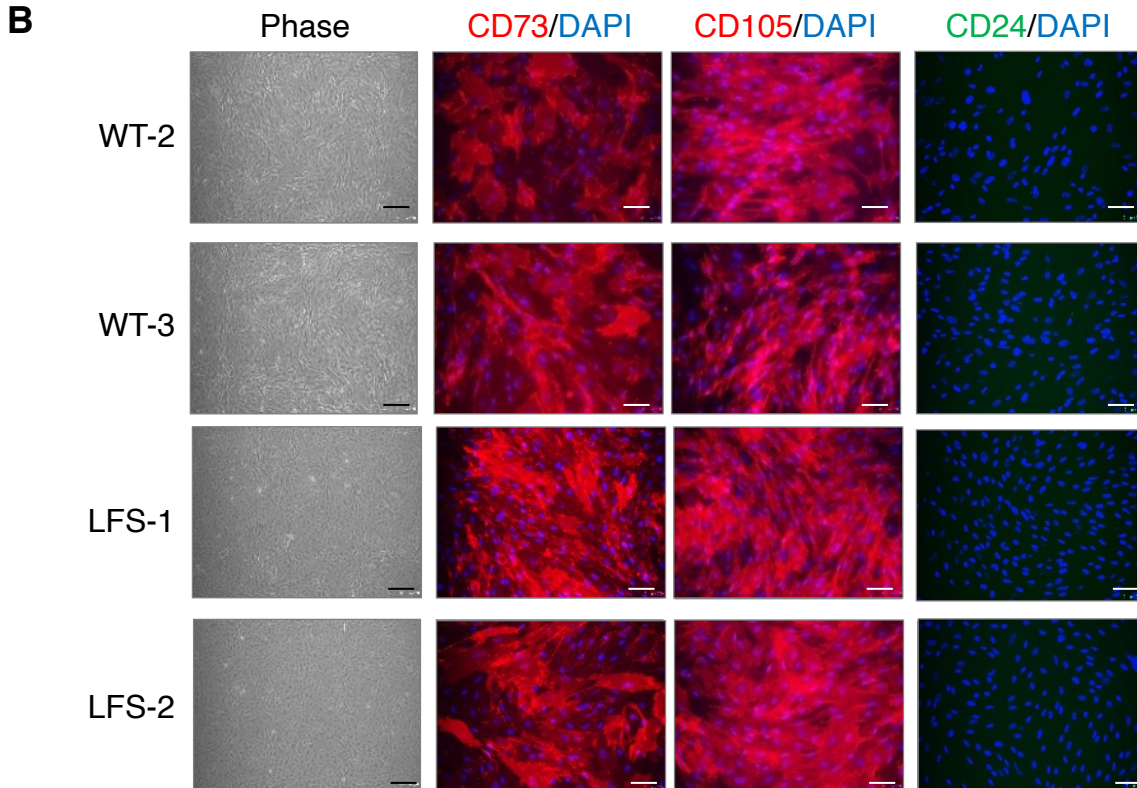
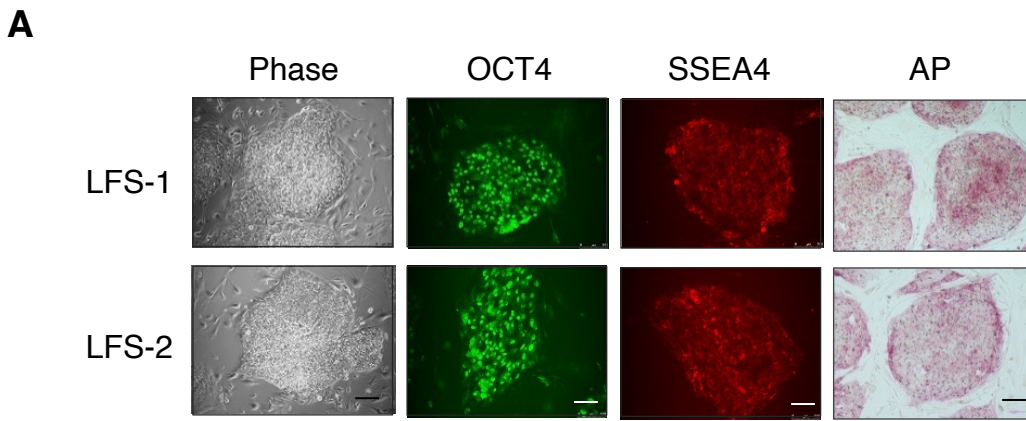
Supplementary Figure S8. Pifithrin- μ disrupts p53(A347D) association with mitochondria and rescues etoposide-mediated cell death

(A) Mitochondrial and cytosolic fractions were isolated from U2OS p53^{AD/AD} cells treated with or without 10 μ M etoposide in the presence or absence of 40 μ M pifithrin- μ for 20 h. Isolated fractions and total cell lysates were subjected to immunoblot analysis with indicated antibodies.

(B) Densitometry analysis of mutant p53 in p53^{AD/AD} U2OS cells associated with mitochondria under indicated conditions normalized to the mitochondrial loading control COX-IV from experiments shown in Fig. 6B (*left*) and Supplementary Fig. S8A (*right*).

(C) Viability of U2OS parental and individual U2OS CRISPR clones varying in p53 status treated with etoposide, PFT μ , and etoposide + PFT μ (B) at indicated concentrations for 48 h was measured via neutral red uptake and normalized to the DMSO control for each cell line. Bars represent mean \pm SEM of three independent experiments (n=3).

(D) Ratios of reduced (GSH) to oxidized (GSSG) glutathione in U2OS parental and U2OS CRISPR cells (p53 KO, p53^{+AD}, and p53^{AD/AD}) grown in low serum conditions with or without 20 μ M etoposide for 24 h.



Supplementary Figure S9. Characterization of LFS iPSCs and MSCs

(A) Single clones of LFS iPSCs (LFS-1 and LFS-2) express hESC pluripotency factor OCT4, hESC surface marker SSEA4, and alkaline phosphatase as visualized by both immunofluorescent and immunohistochemical staining. Scale bars represent 50 μ m.

(B) Single clones of either wild-type (WT-2 and WT-3) or LFS (LFS-1 and LFS-2) MSCs express MSC markers CD73 and CD105 but not pluripotent stem cell marker CD24 as visualized by immunofluorescent staining. Scale bars represent 50 μ m.